

Single Transverse Mode Condition of Lens-Like Strip Waveguide GaInAsP/InP Lasers

KAZUNORI MORIKI AND KENICHI IGA, SENIOR MEMBER, IEEE

Abstract—The theoretical analysis of the single transverse mode condition and lasing properties of a lens-like strip GaInAsP/InP laser is described. First, extended rate equations have been derived which include the carrier diffusion in the active layer and the carrier spread in the cladding layer and the dependency of the carrier lifetime on the current density. Next, it has been shown that the reasonably good assumption that the field of a lasing mode is determined by the built-in index waveguide is effective for simplifying to solve these equations. The result on lasing properties from the theory has been compared with experiments which were made on GaInAsP/InP ($\lambda = 1.3 \mu\text{m}$) lens-like strip and terraced substrate lasers. In addition, the single transverse mode condition is discussed and criteria have been obtained.

I. INTRODUCTION

IT has been observed in stripe geometry gain-guiding lasers that the transverse mode is sometimes unstable and the I - L characteristic has a kink, and these phenomena are explained by the variation of the guiding condition [1]–[7], i.e., it has been made clear that the lasing property of the gain-guiding laser far above the threshold strongly depends on the distribution of light field and carriers in the laser cavity, and this is essential in this type of laser. On the other hand, the mode controlled laser which has a so-called index-guiding structure sustains a relatively stable transverse mode and linear I - L characteristic in the definite range of driving current. When the injection current exceeds the critical level which is the function of the waveguide structure, however, higher transverse modes begin to oscillate and the I - L characteristic begins to exhibit some nonlinearity. Therefore, it is necessary to know how well the laser is operating in single mode by considering, for example, the deformation of the mode field due to the spatial variation of carrier concentration, carrier diffusion in the active layer, the spread of the current in the cladding layer, and so on. Usually, the laser operation including these effects is expressed in terms of the continuous equation of carrier and wave equation [3], [6], [8], and [9]. But, enormous numerical calculation is needed to solve these equations, if we want to have quantitative results which can compare with experimental data. Streifer *et al.* [9] demonstrated by solving the simultaneous differential equations numerically that the theoretical result agrees with the experiment on the range of single mode operation, threshold current level, and differential quantum efficiency. But, it still took

a rather long time to do so by using a computer. In addition, the dependency of a spontaneous carrier lifetime on carrier density was not considered in their analysis, and it was assumed that the waveguide structure of the employed model has an infinite width where many higher modes are far from cutoff.

According to some experiments [10]–[13], on the other hand, it has been shown that the laser with a built-in index waveguide operates with the stable dominant mode in the definite range of the injection level and the mode shape does not change so much. This implies that we can assume that the guided mode itself is determined by the effective index distribution even though some higher modes can be guided in the actual built-in index waveguide (the waveguide is oversize). By taking this into consideration we can expect that the problem is very much simplified and the dependency of the spontaneous carrier lifetime on the carrier density is possibly taken into account without much difficulty.

In this paper we discuss the single mode condition of the lens-like strip waveguide laser and the current range for single mode operation. We provide a theoretical and experimental description of lasing properties of the GaInAsP/InP terraced substrate (TS) laser and the lens-like strip waveguide (LS) laser which have such built-in index waveguides fabricated by a single step LPE [14].

The symbols used in this paper are listed below.

| | |
|--------------------|--|
| A | gain constant |
| $2a$ | waveguide width |
| α | constant which expresses the shape of the waveguide |
| $\Delta\alpha$ | difference of optical modal losses of the fundamental mode and the first mode |
| α_{ab} | absorption loss (due to free carrier absorption, Auger recombination, and other absorptions) in the active layer |
| α_{in} | effective loss when $N(x, y) = 0$ |
| α_{ex} | absorption loss in the cladding layer |
| B_{eff} | effective spontaneous recombination constant |
| c/n_{eff} | propagation constant of the i th mode |
| D | light velocity in the cavity |
| $d(y)$ | diffusion constant of the carrier |
| ξ | thickness of the active layer |
| $G(y, y')$ | confinement factor as a function of y |
| G_i | Green's function of continuous equation |
| I | mode gain of the i th mode |
| I | injection current |
| i_{max} | maximum guided mode number |

Manuscript received March 3, 1982.

K. Moriki was with the Tokyo Institute of Technology, Nagatsuta, Midori-ku, Yokohama, 227, Japan. He is now with the LSI Laboratory, Mitsubishi Electric Corporation, Japan.

K. Iga is with the Tokyo Institute of Technology, Nagatsuta, Midori-ku, Yokohama, 227, Japan.

| | |
|------------------|---|
| k | wave number $2\pi/\lambda$ |
| $K(y, y')$ | integral kernel of the wave equation |
| $\kappa(y)$ | propagation constant along x axis a function of y |
| L | cavity length |
| L_n | diffusion length of carriers |
| $N(x, y)$ | carrier distribution |
| $n(x, y)$ | refractive index |
| P | pumping constant |
| $ \Psi(x, y) ^2$ | normalized light intensity distribution |
| P_{out} | output power from both facets |
| q | charge |
| R | reflective coefficient |
| λ | wavelength |
| R_y | resistance of the cladding layer |
| S_i | photon number associated with the i th transverse mode per unit cavity length |
| τ_s | spontaneous carrier lifetime |
| τ_p | photon lifetime in the cavity |
| W | electrode width. |

II. ANALYSIS

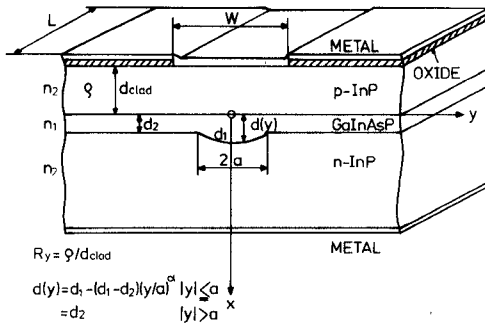
A. Formulation

Prior to the analysis, we will discuss our model. We consider the laser with a three-dimensional strip waveguide as shown in Fig. 1 with a coordinate system. The waveguide in this model is constructed by a nonuniform thickness active layer. Since the refractive index in the active layer reduces with the increase of carrier density, this effect and local gain construct a part of waveguide structure. In addition, if spatial hole burning occurs, the distribution of the gain and the refractive index are disturbed. Streifer *et al.* discussed the influence of the injected carrier levels on the refractive index in the GaAs/GaAlAs laser [9]. The change of refractive index (at 29.4 mW of output versus the threshold) was 0.0025 in their model. This change causes the deformation of the field, and the lasing property may be deteriorated. In our model, on the other hand, we assume that the built-in index waveguide is so strong as we can neglect the change of the refractive index. Since the change of the fundamental mode FWHM was only 4 percent at 2.5 times the threshold as reported in [9], this assumption is reasonably good.

Basic equations which express the rate of changes of N and S_i with respect to time are written as follows:

$$\frac{\partial}{\partial t} N(x, y, t) = D \left(\frac{\partial^2}{\partial x^2} + \frac{\partial^2}{\partial y^2} \right) N(x, y, t) - \frac{1}{\tau_s} N(x, y, t) - (c/n_{\text{eff}}) \sum_{i=0}^{i_{\text{max}}} S_i(t) [A_o N(x, y, t) - \alpha_{in}] \cdot |\Psi_i(x, y)|^2 \quad (1)$$

$$\frac{\partial}{\partial t} S_i(t) = S_i(t) (c/n_{\text{eff}}) \int_{-\infty}^{\infty} dy \int_0^{d(y)} dx [A_o N(x, y, t) - \alpha_{in}] |\Psi_i(x, y)|^2 - \frac{1}{\tau_p} S_i(t) \quad (2)$$



If the overflow of carrier from the other side of the heterojunction can be neglected, another boundary condition is expressed as

$$\frac{\partial}{\partial x} N(x, y, t) \Big|_{x=d(y)} = 0. \quad (5)$$

By integrating (1) with respect to x and substituting the boundary conditions (4) and (5), (1) reduces to a one-dimensional equation with respect to y as follows:

$$\frac{\partial}{\partial t} \bar{N}(y, t) = L_n^2 \frac{\partial^2}{\partial y^2} \bar{N}(y, t) - \bar{N}(y, t) + P(y, t) - (c/n_{\text{eff}}) \sum_{i=0}^{i_{\text{max}}} S_i(t) \frac{\tau_s \xi(y)}{d(y)} \cdot [A_o \bar{N}(y, t) - \alpha_{in}] |\Psi_i(y)|^2 \quad (6)$$

(2) where we have defined

$$\bar{N}(y, t) \equiv \frac{1}{d(y)} \int_0^{d(y)} N(x, y, t) dx \quad (7)$$

$$|\psi_i(y)|^2 \equiv \frac{1}{\xi(y)} \int_0^{d(y)} |\Psi_i(x, y)|^2 dx \quad (8)$$

$$P(y, t) \equiv \tau_s J(y, t) / q d(y) \quad (9)$$

$$L_n \equiv \sqrt{\tau_s D}. \quad (10)$$

$\xi(y)$ is the confinement factor of the field associated with the y direction, and $\bar{N}(y)$ is the average of $N(x, y)$ with respect to the x axis.

The carrier lifetime τ_s depends on the carrier density. After averaging over the y axis, the photon number S_{sp} from spontaneous emission is given by

$$S_{sp} = B_{\text{eff}} \int_{-\infty}^{\infty} \bar{N}(\bar{y})^2 d\bar{y}. \quad (11)$$

In the rate equation (6), the term associated with spontaneous emission is

$$S_{sp} = \frac{\int_{-\infty}^{\infty} \bar{N}(\bar{y}) d\bar{y}}{\tau_s}. \quad (12)$$

By using (11) and (12), the carrier lifetime is determined by the following equation:

$$\tau_s^{-1} = B_{\text{eff}} \frac{\int_{-\infty}^{\infty} \bar{N}(\bar{y})^2 d\bar{y}}{\int_{-\infty}^{\infty} \bar{N}(\bar{y}) d\bar{y}}. \quad (13)$$

This equation exhibits the dependence of τ_s on the carrier concentration.

The parameter $d(y)$ is the thickness of the active layer as a function of the position y , and it is assumed to be expressed as the following equation:

$$\begin{aligned} d(y) &= d(0) - (d(0) - d(a)) (y/a)^{\alpha} & |y| \leq a \\ &= d(a) & |y| > a \end{aligned} \quad (14)$$

where $d(0)$ and $d(a)$ denote the thickness at the center of the waveguide and flat areas of the active layer, respectively, and α is the constant which expresses the shape of the waveguide.

Equations (2) and (6) are extended rate equations including carrier diffusion. We will discuss later on the lasing property of the laser at the steady-state by using these equations. The flow chart for the analysis in this paper is shown in Fig. 2.

B. The Single Mode Condition of the Waveguide

In order to obtain single transverse mode operation, it is desirable to fabricate a single mode waveguide. In this section we discuss the field and the single mode condition of the built-in index waveguide which has already been shown in Fig. 1.

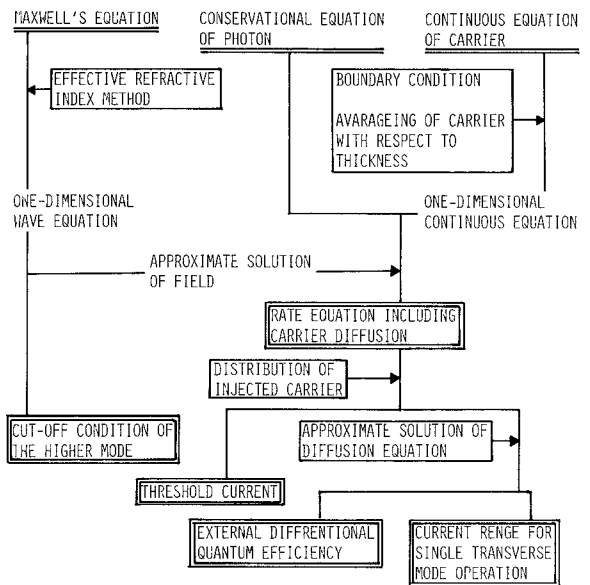


Fig. 2. A flow chart of the analysis where employed assumptions and approximations are marked.

By employing the effective refractive index method [14], (3) can be reduced to

$$\frac{d^2}{d\bar{y}^2} \psi(\bar{y}) - \Gamma^2 \psi(\bar{y}) + V_y^2 (1 - \bar{y}^\alpha) \psi(\bar{y}) = 0 \quad |\bar{y}| \leq 1$$

$$\frac{d^2}{d\bar{y}^2} \psi(\bar{y}) - \Gamma^2 \psi(\bar{y}) = 0 \quad |\bar{y}| > 1 \quad (15)$$

where

$$\bar{y} = y/a \quad (16)$$

$$V_y^2 = a^2 (\kappa(1)^2 - \kappa(0)^2) \quad (17)$$

$$\Gamma^2 = a^2 (\beta_i^2 - k^2 n_1^2 + \kappa(1)^2) \quad (18)$$

and $\kappa(\bar{y})$ satisfies the eigenvalue equation for a boundary condition of the x axis, which is given by

$$\tan(\frac{1}{2} \kappa(\bar{y}) d(\bar{y})) = \sqrt{k^2 (n_1^2 - n_2^2) / \kappa(\bar{y})^2 - 1}. \quad (19)$$

The field equation (9) satisfies boundary conditions written as

$$\frac{d}{d\bar{y}} \psi(\bar{y}) \Big|_{\bar{y}=0} = 0, \quad \frac{d}{d\bar{y}} \psi(\bar{y}) \Big|_{\bar{y}=1} + \Gamma \psi(\bar{y}) \Big|_{\bar{y}=1} = 0 \quad (20)$$

for odd modes, or

$$\psi(\bar{y}) \Big|_{\bar{y}=0} = 0, \quad \frac{d}{d\bar{y}} \psi(\bar{y}) \Big|_{\bar{y}=1} + \Gamma \psi(\bar{y}) \Big|_{\bar{y}=1} = 0 \quad (21)$$

for even modes. These equations are Sturm-Liouville boundary problems. By using the Green's function, they can be transformed to the equivalent Fredholm's integral equation of the first kind

$$\psi'(\bar{y}) = V_y^2 \int_0^1 K(\bar{y}, \bar{y}') \psi'(\bar{y}') d\bar{y}' \quad (22)$$

$$K(\bar{y}, \bar{y}') = \begin{cases} \frac{1}{2\Gamma} \sqrt{1 - \bar{y}^\alpha} \sqrt{1 - \bar{y}'^\alpha} \\ \cdot \{ \exp(-\Gamma|\bar{y} - \bar{y}'|) - \exp(-\Gamma(\bar{y} + \bar{y}')) \} \\ \text{for odd modes} \\ \frac{1}{2\Gamma} \sqrt{1 - \bar{y}^\alpha} \sqrt{1 - \bar{y}'^\alpha} \\ \cdot \{ \exp(-\Gamma|\bar{y} - \bar{y}'|) + \exp(-\Gamma(\bar{y} + \bar{y}')) \} \\ \text{for even modes} \end{cases} \quad (23)$$

where the integral kernel is symmetrized, and

$$\psi'(\bar{y}) = \sqrt{1 - \bar{y}^\alpha} \psi(\bar{y}).$$

The relation between the propagation constant

$$(\beta_i = \sqrt{\Gamma^2/a^2 + k^2 n_1^2 - \kappa^2(1)})$$

and the normalized waveguide width V_y can be derived from eigenvalues of this equation. At the cutoff of the i th mode, the propagation constant is expressed as

$$\beta_i = \lim_{\Gamma \rightarrow 0} \sqrt{\Gamma^2/a^2 + k^2 n_1^2 - \kappa^2(1)} = \sqrt{k^2 n_1^2 - \kappa^2(1)}. \quad (24)$$

Therefore, the condition for a single mode guidance can be obtained by the lowest eigenvalue of (22) and (23) for even modes [15]. Since the kernel is symmetric, the lowest eigenvalue of this equation is given by the approximation of the second order trace by the following:

$$V_{yc}^{-4} = \int_0^1 d\bar{y} \int_0^1 d\bar{y}' K_c(\bar{y}, \bar{y}') K_c(\bar{y}, \bar{y}'). \quad (25)$$

At cutoff a kernel $K_c(\bar{y}, \bar{y}')$ for even modes is given by

$$K_c(\bar{y}, \bar{y}') = \lim_{\Gamma \rightarrow 0} K(\bar{y}, \bar{y}') \\ \begin{cases} \bar{y} \sqrt{1 - \bar{y}^\alpha} \sqrt{1 - \bar{y}'^\alpha} & 0 \leq \bar{y} < \bar{y}' \leq 1 \\ \bar{y}' \sqrt{1 - \bar{y}^\alpha} \sqrt{1 - \bar{y}'^\alpha} & 0 \leq \bar{y} < \bar{y}' \leq 1. \end{cases} \quad (26)$$

Then the cutoff V_y value is given by the following equation for α class waveguide.

$$V_{yc}^{-4} = \left\{ \frac{1}{6} + \frac{1}{\alpha+2} - \frac{3}{\alpha+3} + \frac{4}{3} \times \frac{1}{\alpha+4} \right\}. \quad (27)$$

This equation expresses a single mode condition of the waveguide. The field in the waveguide and the propagation constant can be calculated by eigenfunction and eigenvalue of (22), respectively.

C. Threshold Current

The threshold current of the laser with a lens-like strip waveguide is led from (2) and (6). In order to include the contribution of the current spread to the carrier concentration profile, we utilize the injected carrier distribution which is represented by an exponential function according to Tsang [16],

$$P(\bar{y}) = \begin{cases} \tilde{P} & |\bar{y}| \leq \frac{1}{2} \bar{W} \\ \tilde{P} \exp \left\{ -\frac{\bar{y} - 1/2\bar{W}}{l_o} \right\} & |\bar{y}| > \frac{1}{2} \bar{W} \end{cases} \quad (28)$$

where

$$\tilde{P} = \frac{\tau_s J(0)}{qd(0)}$$

$$l_o = \left(\frac{2}{\delta P_y a^2 J(0)} \right)^{1/2}$$

$$\delta = \frac{q}{kT}$$

$$\bar{W} = W/a.$$

The total current I is given by

$$I = \frac{qd(0) L \bar{W} \tilde{P}}{\tau_s} + 2L \left(\frac{2qd(0) \tilde{P}}{\delta R_y \tau_s} \right)^{1/2} \quad (29)$$

where L is the cavity length, W is the electrode width, and R_y is resistance along the y direction which is represented by $R_y = \rho/d_{\text{clad}}$.

We can assume that the number of photons in the waveguide below the threshold is so small that we can neglect it. From the solution of the differential equation (6) with the assumption that $S_i = 0$ the carrier distribution profile is expressed by the following equations:

$$\bar{N}_o(\bar{y}) = \begin{cases} \tilde{P} - \tilde{P} \left(\frac{\bar{L}_n}{l_o + \bar{L}_n} \right) \exp \left(-\frac{2\bar{W}}{\bar{L}_n} \right) \cosh \left(\frac{\bar{y}}{\bar{L}_n} \right) & \bar{y} \leq \frac{1}{2} \bar{W} \\ \tilde{P} \left(\frac{1^2}{l_o^2 - \bar{L}_n^2} \right) \exp \left(-\frac{\bar{y} - 1/2\bar{W}}{\bar{L}_n} \right) \\ - \frac{1}{2} \tilde{P} \left\{ \left(\frac{\bar{L}_n}{l_o - \bar{L}_n} \right) + \left(\frac{\bar{L}_n}{l_o + \bar{L}_n} \right) \right. \\ \left. \cdot \exp \left(-\frac{\bar{W}}{\bar{L}_n} \right) \right\} \exp \left(\frac{\bar{y} - 1/2\bar{W}}{\bar{L}_n} \right) & |\bar{y}| > \frac{1}{2} \bar{W} \end{cases} \quad (30)$$

where

$$\bar{L}_n = L_n/a. \quad (31)$$

On the other hand, the photon lifetime τ_p in (2) is given by

$$\tau_p^{-1} = \frac{c}{n_{\text{eff}}} \left\{ \frac{1}{L} \ln \frac{1}{R} + \xi_x \alpha_{ab} + (1 - \xi_x) \alpha_{ex} \right\} \quad (32)$$

where

$$\xi_x = \int_{-\infty}^{\infty} \xi(\bar{y}) |\psi(\bar{y})|^2 d\bar{y}. \quad (33)$$

The threshold current is obtained by substituting \tilde{P}_{th} which satisfies (2), (13), (30)–(32), into (29)

$$I_{\text{th}} = LW \left[J_e + \frac{2\sqrt{2}}{\delta R_y W} \sqrt{J_e} \right] \quad (34)$$

where

$$J_e = \frac{\tau_s P_{\text{th}}}{qd(0)}.$$

D. Differential Quantum Efficiency

The output light power of the fundamental mode ($i = 0$) is derived by using (6), which can be transformed into an

$$S_0 = \frac{\int_{-\infty}^{\infty} \int_{-\infty}^{\infty} G(\bar{y}, \bar{y}') P(\bar{y}') \xi(\bar{y}) |\psi_0(\bar{y})|^2 d\bar{y}' d\bar{y} - \int_{-\infty}^{\infty} \bar{N}_{\text{th}}(\bar{y}) \xi(\bar{y}) |\psi_0(\bar{y})|^2 d\bar{y}}{\int_{-\infty}^{\infty} \int_{-\infty}^{\infty} \xi(\bar{y}') \xi(\bar{y}) / d(\bar{y}) G(\bar{y}, \bar{y}') (A_o \bar{N}_{\text{th}}(\bar{y}') - \alpha_{in}) |\psi_0(\bar{y}')|^2 |\psi_0(\bar{y})|^2 d\bar{y}' d\bar{y}}. \quad (41)$$

integral equation

$$\begin{aligned} \bar{N}(\bar{y}) = & \int_{-\infty}^{\infty} G(\bar{y}, \bar{y}') P(\bar{y}') d\bar{y}' \\ & - S_0 \int_{-\infty}^{\infty} G(\bar{y}, \bar{y}') (A_o \bar{N}(\bar{y}') - \alpha_{in}) \frac{\xi(\bar{y})}{d(\bar{y})} \\ & \cdot |\psi_0(\bar{y}')|^2 d\bar{y}' \end{aligned} \quad (35)$$

where $G(\bar{y}, \bar{y}')$ is a Green's function which satisfies the next equation

$$\bar{L}_n^2 \frac{d^2}{d\bar{y}^2} G(\bar{y}, \bar{y}') - G(\bar{y}, \bar{y}') = -\delta(\bar{y} - \bar{y}'). \quad (36)$$

While the mode gain of the fundamental mode is given by

$$G_0 = \int_{-\infty}^{\infty} [A_o \bar{N}(\bar{y}) - \alpha_{in}] \xi(\bar{y}) |\psi_1(\bar{y})|^2 d\bar{y}. \quad (37)$$

Since the mode gain of the lasing mode above the threshold is kept almost constant at the fixed value which corresponds to the mode loss in the cavity, this equation can satisfy, by using $\bar{N}(\bar{y})$ in (35) above, the threshold instead of using $\bar{N}_{\text{th}}(\bar{y})$. Then, the next equation is obtained

$$\begin{aligned} & \int_{-\infty}^{\infty} \bar{N}(\bar{y}) \xi(\bar{y}) |\psi_0(\bar{y})|^2 d\bar{y} \\ & = \int_{-\infty}^{\infty} \bar{N}_{\text{th}}(\bar{y}) \cdot \xi(\bar{y}) |\psi_0(\bar{y})|^2 d\bar{y} \end{aligned} \quad (38)$$

where $\bar{N}_{\text{th}}(\bar{y})$ is the carrier distribution at the threshold. By substituting (35) into (38), we obtain after some algebraic manipulation

$$S_0 = \frac{\int_{-\infty}^{\infty} \int_{-\infty}^{\infty} G(\bar{y}, \bar{y}') P(\bar{y}') \xi(\bar{y}) |\psi_0(\bar{y})|^2 d\bar{y}' d\bar{y} - \int_{-\infty}^{\infty} \bar{N}_{\text{th}}(\bar{y}) \xi(\bar{y}) |\psi_0(\bar{y})|^2 d\bar{y}}{\int_{-\infty}^{\infty} \int_{-\infty}^{\infty} (\xi(\bar{y}') \xi(\bar{y}) / d(\bar{y})) G(\bar{y}, \bar{y}') (A_o \bar{N}(\bar{y}') - \alpha_{in}) |\psi_0(\bar{y}')|^2 |\psi_0(\bar{y})|^2 d\bar{y}' d\bar{y}}. \quad (39)$$

Here, if the spatial hole burning is not so appreciable, $\bar{N}(\bar{y})$ in the denominator of (39) can be replaced by $\bar{N}_{\text{th}}(\bar{y})$,

$$\begin{aligned} & \int_{-\infty}^{\infty} d\bar{y} \int_{-\infty}^{\infty} d\bar{y}' \frac{\xi(\bar{y}') \xi(\bar{y})}{d(\bar{y})} G(\bar{y}, \bar{y}') (A_o \bar{N}(\bar{y}') - \alpha_{in}) \\ & \cdot |\psi_0(\bar{y})|^2 |\psi_0(\bar{y}')|^2 \approx \int_{-\infty}^{\infty} d\bar{y} \int_{-\infty}^{\infty} d\bar{y}' \frac{\xi(\bar{y}') \xi(\bar{y})}{d(\bar{y})} \\ & \cdot G(\bar{y}, \bar{y}') (A_o \bar{N}_{\text{th}}(\bar{y}') - \alpha_{in}) |\psi_0(\bar{y})|^2 |\psi_0(\bar{y}')|^2. \end{aligned} \quad (40)$$

By using this assumption, (39) can be transformed into a closed form

This equation gives the photon number of the lasing mode per unit length of the cavity. The output power P_{out} from both facets is represented by

$$\begin{aligned} P_{\text{out}} &= \hbar \omega \frac{1}{\tau_{pm}} S_0 L \\ &= \hbar \omega S_0 (c/n_{\text{eff}}) \ln \frac{1}{R}. \end{aligned} \quad (42)$$

After numerical calculation with (28)–(30), (41), and (42), the I - L characteristic is obtained. The differential quantum efficiency is given by

$$\begin{aligned} \eta_d &= \frac{dP_{\text{out}}}{dI} \frac{q}{\hbar \omega} \\ &= \frac{dS_0 q (c/n_{\text{eff}}) \ln 1/R}{dI}. \end{aligned} \quad (43)$$

E. The Current Range for Single Transverse Mode Operation

The mode gain G_1 of the first mode is given by

$$G_1 = \int_{-\infty}^{\infty} (A_o \bar{N}(\bar{y}) - \alpha_{in}) \xi(\bar{y}) |\psi_1(\bar{y})|^2 d\bar{y} \quad (44)$$

where $|\psi_1(\bar{y})|^2$ is the field intensity of the first mode. If the difference of modal loss between the fundamental mode and the first mode is written as $\Delta\alpha$, the lasing condition of the first mode is given by

$$G_1 = G_0 + \Delta\alpha. \quad (45)$$

This equation (45) is transformed by using (37) and (44), into

$$\begin{aligned} & \int_{-\infty}^{\infty} \bar{N}(\bar{y}) \xi(\bar{y}) |\psi_1(\bar{y})|^2 d\bar{y} \\ &= \int_{-\infty}^{\infty} \bar{N}_{th}(\bar{y}) \xi(\bar{y}) |\psi_0(\bar{y})|^2 d\bar{y} + \Delta \alpha / A_o. \end{aligned} \quad (46)$$

Here we assume that the deformation of the injected carrier distribution above the threshold of the fundamental mode is not so remarkable. The injected carrier $P(\bar{y})$ at the threshold of the first mode is expressed by

$$P(\bar{y}) = HP_{th}(\bar{y}) \quad (47)$$

where H means the ratio of the pumping constant of the first mode to the fundamental mode at the threshold. By the substitution of (35), (41), and (47) into (46), H at the threshold of the first mode is obtained by

$$H = \frac{\int_{-\infty}^{\infty} \bar{N}_{th}(\bar{y}) \xi(\bar{y}) |\psi_0(\bar{y})|^2 d\bar{y} - \int_{-\infty}^{\infty} \bar{N}_{th}(\bar{y}) \xi(\bar{y}) |\psi_1(\bar{y})|^2 d\bar{y} + \Delta \alpha / A_o}{\int_{-\infty}^{\infty} \bar{N}_{th}(\bar{y}) \xi(\bar{y}) |\psi_1(\bar{y})|^2 d\bar{y} - \int_{-\infty}^{\infty} \bar{N}_{th}(\bar{y}) \xi(\bar{y}) |\psi_0(\bar{y})|^2 d\bar{y} \times \left\{ \begin{array}{l} \int_{-\infty}^{\infty} \int_{-\infty}^{\infty} G(\bar{y}, \bar{y}') (A_o \bar{N}_{th}(\bar{y}') - \alpha_{in}) \xi(\bar{y}) \xi(\bar{y}') |\psi_0(\bar{y})|^2 |\psi_1(\bar{y}')|^2 d\bar{y} d\bar{y}' \\ \int_{-\infty}^{\infty} \int_{-\infty}^{\infty} G(\bar{y}, \bar{y}') (A_o \bar{N}_{th}(\bar{y}') - \alpha_{in}) \xi(\bar{y}) \xi(\bar{y}') |\psi_0(\bar{y})|^2 |\psi_0(\bar{y}')|^2 d\bar{y} d\bar{y}' \end{array} \right\}} \quad (48)$$

where the threshold current of the first mode is given by

$$I_{th1} = \frac{qd(0) L W H \tilde{P}_{th}}{\tau_s} + 2L \left(\frac{2qd(0) H \tilde{P}_{th}}{\delta R_y \tau_s} \right)^{1/2}. \quad (49)$$

III. EXPERIMENTAL AND NUMERICAL RESULTS

In this section we discuss the comparison between numerical and experimental results. Two types of GaInAsP/InP lasers ($\lambda = 1.3 \mu\text{m}$) have been prepared in this work. One is a terraced substrate (TS) laser and the other is a lens-like strip active layer (LS) laser. These lasers have a built-in index waveguide which consists of the partially nonuniform thickness active layer and are almost equivalent to the model in our theory.

First we discuss the criterion for single mode guidance. It can be obtained from (17), (19), and (27) by numerical calculation, i.e., “ a ” in (17) is determined by substituting $\kappa(0)$, $\kappa(1)$, and V_y in (17) which are obtained from (19) and (27). The result is shown in Fig. 3, where $n_1 = 3.52$ and $n_2 = 3.2$ are used as the refractive indexes of the GaInAsP active layer and InP at $1.3 \mu\text{m}$ wavelength [17], respectively, and $\alpha = 2$. The dimension of the waveguide fabricated by LPE growth is located within a shadowed region in Fig. 3, which has $2.5\text{--}3 \mu\text{m}$ in width and thickness difference by about $0.5 \mu\text{m}$. Single transverse mode operation has been obtained with these lasers in the range from 1.3 to 3 times the threshold.

Threshold current can be calculated from (2), (29), (30), (32), and (13). First we obtain P from (30), which satisfies (2), where τ_p and the field are given by (32) and (A1), respectively. Next by using this \tilde{P} , we substitute (30) into (13), so that τ_s is given. We again obtain \tilde{P} which satisfies (2) by using τ_s . This process is continued until \tilde{P} converges, and thus

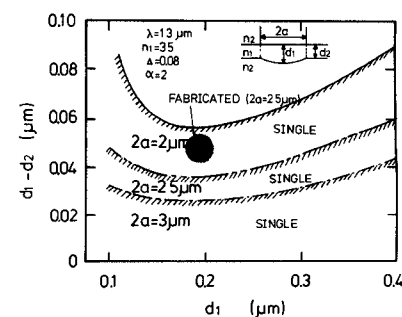


Fig. 3. Single mode condition for a lens-like strip waveguide.

\tilde{P}_{th} is determined. The threshold current I_{th} is calculated by substituting \tilde{P}_{th} into (29).

Here the gain constant A_o and α_{in} at $1.3 \mu\text{m}$ and $1.6 \mu\text{m}$ were reported by Yano *et al.* [18] and Stubkjaer *et al.* [19],

respectively. We use $A_o = 1.6 \times 10^{-16} \text{ cm}^2$ and $\alpha_{in} = 230 \text{ cm}^{-1}$ after [18]. The effective spontaneous recombination constant B_{eff} for GaInAsP ($\lambda = 1.6 \mu\text{m}$) was measured as $1.2 \times 10^{-10} \text{ cm}^3 \cdot \text{s}^{-1}$ [19]. We have assumed that $B_{eff} = 2 \times 10^{-10} \text{ cm}^3 \cdot \text{s}^{-1}$. $D = 30 \text{ cm}^2 \cdot \text{s}^{-1}$ have been used as the diffusion constant. The other parameter values are taken to be $\alpha_{ex} = 20 \text{ cm}^{-1}$, $\alpha_{ab} = 40 \text{ cm}^{-1}$, and $R = 0.31$. The result of the computer calculation is shown in Fig. 4.

The dimensions of the TS laser used in the measurement are as follows: the active layer is $0.17 \mu\text{m}$ thick at center and $0.05 \mu\text{m}$ thick at flat areas, InP cladding layer is $2.5 \mu\text{m}$ thick (Zn doped $5 \times 10^{17} \text{ cm}^{-3}$), and GaInAsP cap layer is $0.5 \mu\text{m}$ thick (Zn doped). Measured data at the pulsed operation are shown by the dots in Fig. 4. The resistivity is estimated as $\rho_y = 3 - 6 \times 10^{-2} \Omega \cdot \text{cm}$ with $\rho_y = 1/q\mu p$, where μ is about $3 \times 10^2 \text{ cm}^2 \cdot \text{V}^{-1} \cdot \text{s}$ [20] and $p = 0.5 - 1 \times 10^{18} \text{ cm}^{-3}$. The result of the calculation is shown by the solid lines, which agree with the measurement. The nonlinearity of the theoretical lines in shorter cavity length is caused by the dependency of τ_s on the carrier concentration. Results for LS GaInAsP/InP lasers are shown in Fig. 5. The same parameters are used for calculation.

The threshold current versus the waveguide width $2a$ for several R_y are shown in Fig. 6. A shadowed region in this figure shows the area of parameters in the experiment. With larger R_y , the threshold current level reduces. But, if R_y is larger than 1000Ω , it is not so sensitive. Therefore, it is one of the criteria for the design of lasers that R_y is made to be greater than 1000Ω . This value may be achieved when p (dopant concentration) $\times d_{clad}$ (cladding layer thickness) $< 3.2 \times 10^{-14} \text{ cm}^{-2}$.

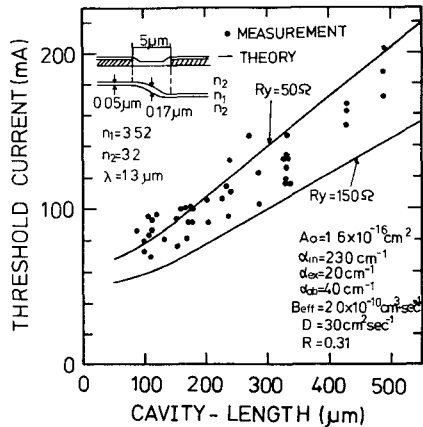


Fig. 4. Threshold current versus cavity length for GaInAsP/InP TS lasers.

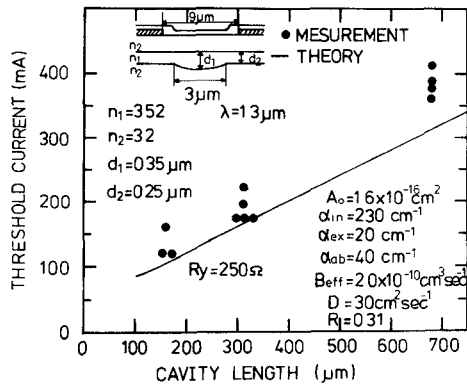


Fig. 5. Threshold current versus cavity length for GaInAsP/InP lens-like strip active layer (LS) lasers.

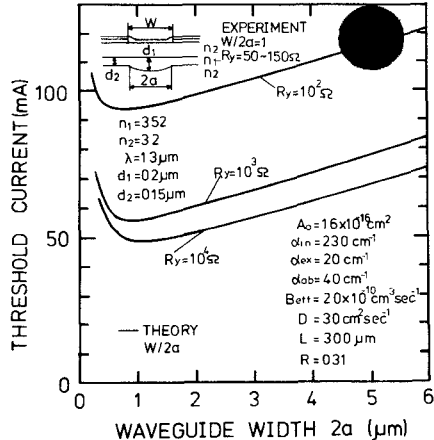


Fig. 6. Threshold current versus waveguide width for the GaInAsP/InP laser with a nonuniform thickness active layer.

From Fig. 6 the expected minimum threshold current is about 50 mA for the waveguide of 1-2 μm in width and 300 μm cavity length. This value is large as compared with BH structure lasers. This is caused by the spread of injected current in the cladding layer and the carrier diffusion in the active layer. It is desirable for the low current operation to fabricate the waveguide of 2-3 μm in width.

The threshold current of the first mode is calculated from (49), where \tilde{P}_{th} and $N_{th}(y)$ are the injected carrier and the carrier density in the active layer at a threshold of the funda-

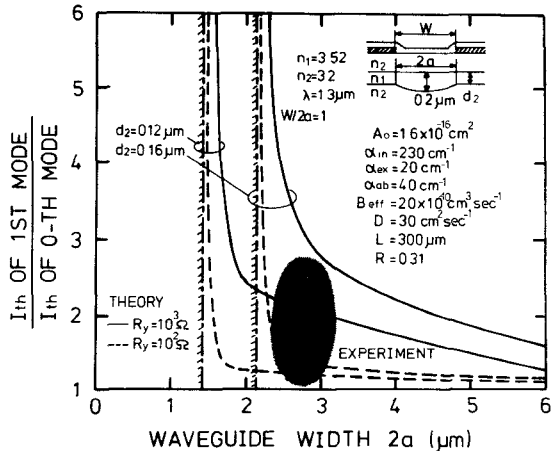


Fig. 7. Criteria for a single mode operation of GaInAsP/InP with a non-uniform thickness active layer.

mental mode, respectively. When the threshold current of the fundamental mode is calculated in Section II-C, these values are obtained. The difference of optical loss between the fundamental mode and the first mode, which is expressed by $\Delta\alpha$, includes a scattering loss due to the imperfection of a waveguide, etc. Since the modal loss of the first mode is usually larger than that of the fundamental mode, $\Delta\alpha$ is positive. Here, we present the result for $\Delta\alpha = 0$. This assumption is severer for the single mode condition than for the case of $\Delta\alpha > 0$. Fig. 7 shows the current range for the single mode operation versus the waveguide width $2a$. The first higher order mode is cut off in the left shadowed areas of the broken line. It is found from this figure that the criteria have a margin for design of single transverse mode lasers. Experimental results are shown by the shaded area in Fig. 7.

IV. CONCLUSION

A laser with the nonuniform thickness strip waveguide is one of desirable devices for single transverse mode operation. We have discussed properties of this type of lasers and the single mode condition by introducing the theory based on extended rate equations. In addition we have compared the result of calculation with experiments which have been made for GaInAsP/InP lasers ($\lambda = 1.3 \mu\text{m}$). The p (dopant concentration in cladding layer) $\times d_{\text{clad}}$ (cladding layer thickness) $< 3.2 \times 10^{-14} \text{ cm}^{-2}$, and waveguide width ($2a$) = 2-3 μm are necessary to make threshold current reasonably low. The criteria of the design for the single transverse mode operation have some margin compared to that for the passive waveguide.

APPENDIX

The next field equation is used in the numerical calculation of the sections

$$\psi_0(\bar{y}) = \begin{cases} \psi_0 \cos(f(\bar{y})) & \{\bar{y}|_{f(\bar{y})} \geq 0\} \\ \psi_0 \exp(-g(\bar{y})) & \{\bar{y}|_{g(\bar{y})} \geq 0\} \end{cases} \quad (A1)$$

for the fundamental mode,

$$\psi_1(\bar{y}) = \begin{cases} \psi_1 \sin(f(\bar{y})) & \{\bar{y}|_{f(\bar{y})} \geq 0\} \\ \psi_1 \exp(-g(\bar{y})) & \{\bar{y}|_{g(\bar{y})} \geq 0\} \end{cases} \quad (A2)$$

or the first higher mode, where

$$\frac{d}{d\bar{y}} f(\bar{y}) = \sqrt{k^2 n_1^2 - \kappa(\bar{y})^2 - \beta_i^2} \quad (A3)$$

$$\frac{d}{d\bar{y}} g(\bar{y}) = \sqrt{\beta_i^2 + \kappa(\bar{y})^2 - k^2 n_1^2}.$$

The propagation constant is obtained by the second order trace of (22) and (23). These are better approximations than the WKB method near the cutoff.

$$V_y^{-4} = \int_0^1 d\bar{y} \int_0^1 d\bar{y}' K(\bar{y}, \bar{y}') K(\bar{y}', \bar{y}). \quad (A4)$$

ACKNOWLEDGMENT

The authors would like to thank Prof. Y. Suematsu of Tokyo Institute of Technology for discussion. They also wish to thank Dr. Y. Kokubun for discussion about the cutoff condition of the waveguide and Dr. K. Wakao for experiments.

REFERENCES

- [1] T. L. Paoli, "Nonlinearities in the emission characteristics of stripe-geometry (AlGa)As double heterostructure junction lasers," *IEEE J. Quantum Electron.*, vol. QE-12, pp. 770-776, Dec. 1976.
- [2] K. Kobayashi, R. Lang, H. Yonezu, I. Sakuma, and I. Hayashi, "Horizontal mode deformation and anomalous lasing properties of stripe geometry injection lasers: Experiment," *Japan. J. Appl. Phys.*, vol. 1, pp. 207-208, Jan. 1977.
- [3] N. Chinone, "Nonlinearity in power-output-current characteristics of stripe-geometry injection lasers," *J. Appl. Phys.*, vol. 48, pp. 3237-3243, 1977.
- [4] P. A. Kirkby and A. R. Selway, "Observations of self-focusing in stripe geometry semiconductor lasers and the development of a comprehensive model of their operation," *IEEE J. Quantum Electron.*, vol. QE-13, Aug. 1977.
- [5] G.H.B. Thompson, D. F. Lovelace, and S.E.M. Turley, "Kinks in the light/current characteristics and near field shifts in (GaAl)As heterostructure stripe lasers and their explanation by the effect of self-focusing on a built-in optical waveguide," *Inst. Elec. Eng. Solidstate Elect. Dev.*, vol. 2, pp. 12-30, 1978.
- [6] R. Lang, "Lateral transverse mode instability and its stabilization in stripe geometry injection lasers," *IEEE J. Quantum Electron.*, vol. QE-15, pp. 718-746, Aug. 1979.
- [7] P. M. Asbeck, D. A. Cammack, J. J. Daniele, and V. Kelbanoff, "Lateral mode behavior in narrow stripe lasers," *IEEE J. Quantum Electron.*, vol. QE-15, pp. 727-733, Aug. 1979.
- [8] J. Buus, "A model for static properties of DH lasers," *IEEE J. Quantum Electron.*, vol. QE-15, pp. 734-739, Aug. 1979.
- [9] W. Streifer, R. D. Burnham, and D. R. Scifres, "Channeled substrate nonplanar laser analysis—Part 1: Formulation and the plano-convex waveguide laser," *IEEE J. Quantum Electron.*, vol. QE-17, pp. 736-744, May 1981.
- [10] T. Tsukada, "GaAs-Ga_{1-x}Al_xAs BH injection lasers," *J. Appl. Phys.*, vol. 45, pp. 4899-4906, 1974.
- [11] H. Namizaki, H. Kan, M. Ishii, and R. Ito, "Transverse-junction-stripe geometry DH lasers with very low threshold current," *J. Appl. Phys.*, vol. 45, pp. 2785-2786, 1974.
- [12] K. Aiki, M. Nakamura, T. Kuroda, and I. Umeda, "Channeled substrate-planar structure (AlGa)As injection lasers," *Appl. Phys. Lett.*, vol. 48, pp. 645-651, June 1977.
- [13] T. Sugino, M. Wada, H. Shimizu, K. Itoh, and I. Teramoto, "Terraced-substrate GaAs-(GaAl)As injection lasers," *Appl. Phys. Lett.*, vol. 34, pp. 270-272, Feb. 1979.
- [14] K. Moriki, K. Wakao, M. Kitamura, K. Iga, and Y. Suematsu, "Single transverse mode operation of terraced substrate GaInAsP/InP laser at 1.3 μm waveguide," *Japan. J. Appl. Phys.*, vol. 19, pp. 2191-2196, Nov. 1980.
- [15] Y. Kokubun and K. Iga, "Formulas for TE₀₁ cutoff in optical fibers with arbitrary index profile," *J. Opt. Soc. Amer.*, vol. 70, pp. 36-40, Jan. 1980.
- [16] W. T. Tsang, "The effects of lateral current spreading carrier out-diffusion, and optical mode losses on the threshold current density of GaAs-Al_xGa_{1-x}As stripe-geometry DH lasers," *J. Appl. Phys.*, vol. 49, pp. 1031-1044, Mar. 1978.
- [17] R. E. Nahory and M. A. Pollack, "Threshold dependence on active-layer thickness in InGaAsP/InP D.H. lasers," *Electron. Lett.*, vol. 14, pp. 727-729, Nov. 1978.
- [18] Y. Yano, H. Nishi, and M. Takusagawa, "Theoretical and experimental study of the threshold characteristics in InGaAsP/InP DH lasers," *IEEE J. Quantum Electron.*, vol. QE-15, pp. 571-579, July 1979.
- [19] K. Stubkjaer, M. Asada, S. Arai, and Y. Suematsu, "Spontaneous recombination, gain and refractive index variation for 1.6 μm wavelength InGaAsP/InP lasers," *Japan. J. Appl. Phys.*, vol. 20, no. 7, July 1981.
- [20] P. Bhattacharya, J. W. Ku, S.J.T. Qwen, G. H. Olsen, and S. H. Chiao, "LPE and VPE In_{1-x}Ga_xAs_yP_{1-y}/InP transport properties, defects and device consideration," *IEEE J. Quantum Electron.*, vol. QE-17, pp. 150-161, Feb. 1981.



Kazunori Moriki was born in Saitama, Japan, on December 2, 1953. He received the B.S. degree in electrical engineering from Saitama University, Saitama, Japan, in 1977, and the M.S. and Ph.D. degrees in electronics systems from the Tokyo Institute of Technology, Tokyo, Japan, in 1979 and 1982, respectively.

He contributed to GaInAsP/InP single mode laser technology during his Ph.D. study. He joined the Mitsubishi Electric Corporation and is currently working on semiconductor technology at the LSI Laboratory.

Dr. Moriki is a member of the Institute of Electronics and Communication Engineers of Japan and the Japan Society of Applied Physics.

Kenichi Iga (S'67-M'68-SM'80), for a photograph and biography, see p. 29 of the January 1982 issue of the JOURNAL OF QUANTUM ELECTRONICS.